

## ABSORPTION CORRECTIONS IN A MUELLER REGGE ANALYSIS OF INCLUSIVE PHOTO- AND ELECTROPRODUCTION

N.S. CRAIGIE and G. KRAMER

*II. Institut für Theoretische Physik der Universität Hamburg*

Received 4 March 1974

**Abstract:** We discuss the photon fragmentation region of inclusive pion photo- and electroproduction in terms of a helicity dependent Mueller-Regge model, in which cut contributions are taken into account. It is shown that the inadequacies of a pure Regge pole expansion can be corrected if certain types of Regge cut contributions are included. The transition from electro-production to the photo-production limit is shown to be non-smooth in the case of charged pions and we point out that normal triple-Regge mechanisms are unlikely to be important in the deep inelastic region.

### 1. Introduction

In a previous work [1] we carried out a Mueller-Regge analysis of the photon fragmentation region of the inclusive photo- and electroproduction reactions

$$\gamma + p \rightarrow \pi^{\pm} + x, \quad (1)$$

$$\gamma + p \rightarrow \pi^0 + x, \quad (2)$$

in which spin and normality (sometimes referred to as naturality) properties were taken into account. In ref. [1] (hereafter referred to as I) we showed that certain features of the data cannot be explained by Regge poles alone. The situation looks somewhat similar to exclusive photoproduction processes like

$$\gamma + p \rightarrow \pi^+ + n, \quad (3)$$

for which a purely (evasive) Regge pole model [2] would predict, that the cross section vanishes as  $t \rightarrow 0$ . This property is closely related to the correspondence between the linear polarization of the photon and the normality of the Reggeon exchanged sometimes referred to as the Stichel relations [3]. These state that the positive and negative normalities contribute respectively only to  $\sigma_{\perp}$  and  $\sigma_{\parallel}$  (the cross section for perpendicular and parallel polarized photons). Thus for a purely evasive Regge pole, either  $\sigma_{\perp}$  or  $\sigma_{\parallel}$  vanishes and since  $\sigma_{\parallel} - \sigma_{\perp} \propto t$  (as  $t \rightarrow 0$ ) for kinematic reasons, we have a dip in the forward direction (here after referred to as a normality dip). How-

ever experimentally the cross section for (3) is peaked in the forward direction [4] and this has been subsequently understood in terms of Regge cut contributions [5, 6]. In (I) we showed at a heuristic level, that for the inclusive distributions (1) and (2), the same normality arguments lead to the prediction that, if Regge poles are exchanged in the  $\gamma\pi$  channels, then the positive normality poles contribute only to  $\sigma_{\perp}$ , while the negative normality poles contribute only to  $\sigma_{\parallel}$ ,  $\sigma_L$  and  $\sigma_1$ . Further since  $\sigma_{\parallel} - \sigma_{\perp}$  vanishes like  $k_{\perp}^2$  for kinematic reasons, where  $k_{\perp}$  is the transverse momentum of the pion, it follows that the inclusive photoproduction distributions (1) and (2) will vanish as  $k_{\perp} \rightarrow 0$  in a Mueller Regge model, in which only Regge pole contributions are taken into account. Experimentally [7] there is clear evidence against such normality dips in (1) and (2). Infact for (1) the data shows a marked peaking as  $k_{\perp}^2 \rightarrow 0$ , completely analogous to the peak in the exclusive cross section (3). On the other hand, unlike the inclusive case (reaction (2)), there is evidence [4] for such a dip in the case of the exclusive neutral pion photo production reaction

$$\gamma + p \rightarrow \pi^0 + p, \quad (4)$$

which in a Regge pole model would be dominated by  $\omega$ -exchange.

In deriving a Regge representation for an inclusive distribution, one encounters a number of formal problems, which makes it apparent that there are some essential differences between the Reggization of higher point functions as compared with the usual Gribov-Froissart continuation and Regge limit of the four point function. These differences have been elaborated on in the case of spinless particles in a number of papers [8]. The firm basis of the above normality relations for the inclusive distributions has yet to be established. We shall consider the problem elsewhere [9], where we make an attempt at establishing such relations at a somewhat more formal level, namely by deriving a generalized Sommerfeld-Watson type representation of the six-point function from a simplified model of its analyticity, analogous to fixed  $t$ -dispersion relations.

It was also shown in (I), that when  $(-q^2) \gg m_{\pi}^2$  the electroproduction of charged pions, which is dominated by pion exchange, is predominantly longitudinal and that a non-dip structure was expected. The Regge pole model for moderate  $q^2$  (i.e.  $0.1 < |q^2| < 0.5 \text{ GeV}^2$ ) was infact seen to be compatible with the data. However for larger  $(-q^2)$ , due to the dependence on  $q^2$  and  $x$  entering through the pion propagator, the triple-Regge pole contribution becomes more and more compressed in the region near  $x \simeq 1$ . Infact for  $|q^2| \simeq 1 \text{ GeV}^2$ , the pion exchange contributes only to the region  $0.85 < x < 1$ , leaving much of the photon fragmentation region unaccounted for.

Bearing in mind the above points, we attempt in the present work to carry out a Mueller-Regge analysis of the inclusive processes (1) and (2), in which we include the Regge-cut contributions in a helicity dependent framework. The latter is set up in sect. 2 and the specific Regge-cut contributions relevant to processes (1) and (2) are calculated in sect. 3. Although the results in these sections are on heuristic footing, they are adequate from the phenomenological point of view. This is demonstrated in sect. 4, where we compare the resulting model with the data. The kind of Regge-cut

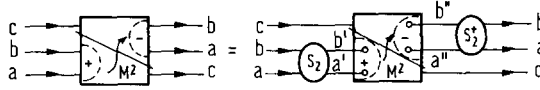


Fig. 1. Rescattering expansion for the Mueller discontinuity formula.

contributions we consider are similar to these considered by Cardy [10] in connection with the renormalization of the triple-Reggeon vertex from the point of view of Gribov's Reggeon calculus. Some details are elaborated on in the appendix.

### 2. Calculation of Regge-cut contributions

In order to incorporate the helicity dependence correctly, it turns out to be convenient to calculate the Regge cut contributions in terms of rescattering effects in the  $s$ -channel fig. 1. For this purpose we work with the  $s$ -channel helicity inclusive structure functions defined by

$$\begin{aligned}
 H^{\lambda'}(p', q'; p, q) = & \sum_{\lambda_p} \sum_{\chi(n, \xi)} \int \sum_{i=1}^n \frac{d^3 k_i}{(2\pi)^3 2k_{i0}} (2\pi)^4 \delta^4 \left( \sum_1^n k_i + k - p - q \right) \\
 & \times \langle k, k_1, \dots, k_n | T | p, \lambda_p; q, \lambda \rangle \langle k, k_1, \dots, k_n | T | p', \lambda_p'; q', \lambda' \rangle^*, \quad (2.1)
 \end{aligned}$$

where in the summation over  $\chi(n, \xi)$ ,  $\xi$  denotes all the unobserved discrete labels involved in the missing mass state  $X$ . In (2.1)  $q, k$  and  $p$  are respectively the momenta of the incoming virtual photon, the outgoing pion and the target proton;  $q'$  and  $p'$  refer to the complex conjugate matrix element and in order that we can write separate partial wave expansions for both the above matrix elements, we allow  $(q, p)$  and  $(q', p')$  to be different, but keep the constraint  $p + q = p' + q'$ .

We shall use  $p + q = p' + q' = 0$  as the reference system and define

$$\begin{aligned}
 q &= (q_0, q \sin \theta \cos \phi, q \sin \theta \sin \phi, q \cos \theta), \\
 q' &= (q_0, q \sin \theta' \cos \phi', q \sin \theta' \sin \phi', q \cos \theta'), \\
 k &= (k_0, 0, 0, k_z), \quad k_l = xq = k_z \cos \theta. \quad (2.2)
 \end{aligned}$$

The variables

$$\begin{aligned}
 \tau &= 2q \sin \frac{1}{2} \theta, \\
 \tau' &= 2q \sin \frac{1}{2} \theta',
 \end{aligned}$$

correspond approximately to the transverse momentum of the observed pion in a system, in which  $q$  is chosen along the  $z$ -axis.  $\tau$  and  $\tau'$  are related to the squared four momentum transfer variables  $t$  and  $t'$  by:

$$t = (k - q)^2 = t_{\min} - \tau^2 x,$$

$$t' = (k - q')^2 = t_{\min} - \tau'^2 x,$$

with

$$t_{\min} = -(1 - x) \left( -q^2 + \frac{m_\pi^2}{x} \right). \tag{2.3}$$

As we are interested in the behaviour of (2.1) in the limit  $k_\perp/\sqrt{s} \rightarrow 0$ , we can make use of the usual small angle high energy approximation. Namely we can convert the partial wave expansions in  $\gamma p$  and  $\gamma' p'$  channels into impact parameter integrals over  $b = J/q$  and  $b' = J'/q'$ , where  $J$  and  $J'$  are respectively the angular momenta in the above two channels. The result is given by (see appendix A)

$$H^{\lambda'\lambda}(\tau', \phi'; \tau, \phi) = \sum_{m=-\infty}^{\infty} \int_0^\infty db' b' \int_0^\infty db b h^{\lambda'\lambda}(b', b; m) e^{i(m+\lambda)\phi} e^{-i(m+\lambda')\phi'}$$

$$\times J_{\lambda+m}(b\tau) J_{\lambda'+m}(b'\tau'). \tag{2.4}$$

$m - \lambda_p$  is the helicity of the intermediate state with missing mass  $M^2$ . The summation over  $m$  includes the average over the proton helicity. The  $b$ -space amplitude  $h^{\lambda'\lambda}(b', b; m)$  is obtained from the inverse of (2.4), which is given by

$$h^{\lambda'\lambda}(b', b; m) = \int_0^{2\pi} \frac{d\phi}{2\pi} \int_0^{2\pi} \frac{d\phi'}{2\pi} \int_0^\infty d\tau \tau \int_0^\infty d\tau' \tau' H^{\lambda'\lambda}(\tau', \phi'; \tau, \phi)$$

$$\times J_{\lambda'+m}(b'\tau') J_{\lambda+m}(b\tau) e^{i(\lambda'+m)\phi'} e^{-i(\lambda+m)\phi}. \tag{2.5}$$

It is convenient to introduce the  $m$ -projection of the inclusive amplitude through

$$H^{\lambda'\lambda}(\tau', \tau; m) = \int_0^\infty dt' t' \int_0^\infty dt t h^{\lambda'\lambda}(b', b; m) J_{\lambda'+m}(b'\tau') J_{\lambda+m}(b\tau), \tag{2.6}$$

so that

$$H^{\lambda'\lambda}(\tau', \phi'; \tau, \phi) = \sum_{m=-\infty}^{\infty} H^{\lambda'\lambda}(\tau', \tau, m) e^{-i(\lambda'+m)\phi'} e^{i(\lambda+m)\phi} \tag{2.7}$$

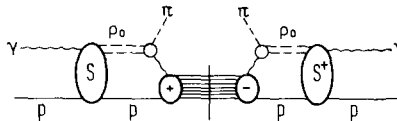


Fig. 2. Rescattering corrections to the Mueller Regge expansion of  $\gamma + p \rightarrow \pi + x$ .

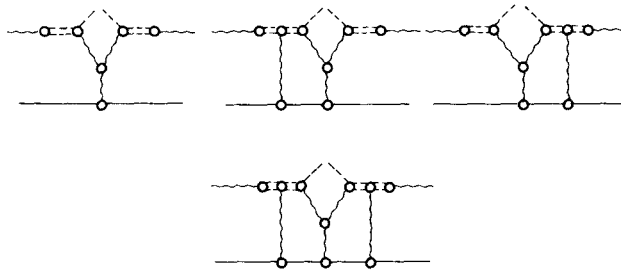


Fig. 3. Reggeon diagram expansion for the triple Regge limit of  $\gamma p \rightarrow \pi x$  (The double dotted line represents the  $\rho^0$ ).

(2.4) to (2.7) define the appropriate impact parameter expansion of the six-point function  $\gamma p \pi \rightarrow \gamma' p' \pi'$ . The Regge cuts can be thought of as absorption corrections to a pure Regge pole expansion of  $\gamma p \pi \rightarrow \gamma' p' \pi'$ . The detailed structure of such an expansion for the forward direction was discussed in (1). The generalizations to the non forward case are left to the next section. Here we assume  $h_R^{\lambda\lambda}(b', b; m)$  has been calculated from (2.5) and  $H_R^{\lambda\lambda}(\tau', \phi; \tau, \phi)$ . Then, following the prescription of ref. [5] for the exclusive case, the rescattering correction to  $H_R^{\lambda\lambda}(b', b; m)$  arising through the intermediate  $\rho^0 p$  state shown in fig. 2, is given by

$$h^{\lambda\lambda}(b', b; m) = \tilde{S}^*(b') h_R^{\lambda\lambda}(b', b; m) \tilde{S}(b), \tag{2.6}$$

where we write  $S(b)$  in the form<sup>†</sup>

$$S(b) = [1 - \frac{1}{2}c e^{-\frac{1}{4}b^2/a}] . \tag{2.7}$$

The second term in  $\tilde{S}(b)$  can represent the  $b$ -space projection of the Pomeron pole contribution, in which case we are lead to the Reggeon diagram shown in fig. 3. However for the purpose of numerical estimates it is convenient also to relate the constants  $c$  and  $a$  directly to the helicity independent  $\rho_0 p$  scattering amplitude  $F(s, t)$  using

$$\text{Im } F(s, t) = \sigma_{\text{tot}}^s e^{at} ,$$

with

$$c = \frac{\sigma_{\text{tot}}}{8\pi a} . \tag{2.8}$$

Using the integrals

<sup>†</sup> An alternative prescription would be that of Gottfried and Jackson, in which the factor  $\tilde{S}(b)$  in (2.7) is replaced by  $[1 - c e^{-b^2/4a}]^{\frac{1}{2}}$ . However this has obvious disadvantages.

$$\int_0^{\infty} db b J_n(b\tau) J_n(b\tau') = \frac{1}{\tau} \delta(\tau' - \tau), \quad (2.9)$$

$$\int_0^{\infty} db b J_n(b\tau) J_n(b\tau') e^{-b^2/4a} = 2a e^{-a(\tau^2 + \tau'^2)} I_n(2a\tau\tau'), \quad (2.10)$$

it is simple to show that

$$\begin{aligned} H^{\lambda'\lambda}(\tau', \tau, m) &= \int_0^{\infty} db' b' \int_0^{\infty} db b \tilde{S}^*(b') h_R^{\lambda'\lambda}(b'; b; m) \tilde{S}(b) J_{\lambda'+m}(b'\tau') J_{\lambda+m}(b\tau) \\ &= \int_0^{\infty} d\tau'_1 \tau'_1 \int_0^{\infty} d\tau_1 \tau_1 H_R^{\lambda'\lambda}(\tau'_1, \tau_1; m) \\ &\quad \times \left\{ \frac{1}{\tau'} \delta(\tau' - \tau'_1) - ca e^{-a(\tau'^2 + \tau_1'^2)} I_{\lambda'+m}(2a\tau'\tau'_1) \right\} \\ &\quad \times \left\{ \frac{1}{\tau} \delta(\tau - \tau_1) - ca e^{-a(\tau^2 + \tau_1^2)} I_{\lambda+m}(2a\tau\tau_1) \right\}. \end{aligned} \quad (2.11)$$

If we insert (2.11) in (2.7), then we can carry out the summation over  $m$  by making repeated use of the addition formula

$$e^{Z \cos \phi} = \sum_{m=-\infty}^{+\infty} e^{im\phi} I_m(Z), \quad (2.12)$$

writing  $d^2\mathbf{\tau} = d\tau d\phi$ , where  $\tau = (\tau \cos \phi, \tau \sin \phi)$  the final result can be written in the form

$$H^{\lambda'\lambda}(\tau, \tau') = \int \frac{d^2\mathbf{\tau}'_1}{2\pi} \int \frac{d^2\mathbf{\tau}_1}{2\pi} S^*(\mathbf{\tau}' - \mathbf{\tau}'_1) H_R^{\lambda'\lambda}(\mathbf{\tau}'_1, \mathbf{\tau}_1) S(\mathbf{\tau} - \mathbf{\tau}_1),$$

where

$$S(\mathbf{\tau} - \mathbf{\tau}_1) = \delta^{(2)}(\mathbf{\tau} - \mathbf{\tau}_1) - ca e^{-a(\tau^2 - \tau_1)^2}. \quad (2.13)$$

The result (2.13) as far as the  $\tau$ -integration structure is concerned, can be derived directly from the Reggeon diagrams in fig. 3 using the method of Rothe [12a]<sup>†</sup> (see appendix B). However the method developed above shows how one can write down the corresponding formula for arbitrary external helicities.

If one uses exponential approximations for Regge residues and linear forms for the Regge trajectory functions, the integrals in (2.13) can be explicitly evaluated. It turns out for our purposes that such approximations are sufficient to show the general effect of the Regge-cut corrections and we shall consider the specific cases we

\* For an application in the present context see [12b].

are interested in, in the next section.

In the small transverse momentum region one can use (2.11), since only a few terms in the  $m$ -summation will be important. In particular the term  $m = -\lambda = -\lambda'$  is the only non-vanishing contribution in the limit  $\tau = \tau' \rightarrow 0$ , in which, for general  $m$ , we have the property

$$H^{\lambda\lambda'}(\tau, \tau, m) \sim \tau^{|\lambda+m|+|\lambda'+m|} \text{ as } \tau \rightarrow 0. \tag{2.14}$$

(2.11) involves only a two dimensional integral instead of the four dimensional integral involved in (2.13), so it could in fact be useful for numerical purposes, when the simplifying assumptions in the next section are not made.

### 3. Evaluation of rescattering formula for $\pi$ - and $\omega$ -exchange

#### 3.1. $\pi$ -exchange

Pion exchange presents a problem, since it is not explicitly gauge invariant. Therefore we must make a gauge invariant extension. We do this by specifying an explicitly gauge invariant covariant which is equal to  $\Gamma_{\alpha'\alpha}^4$ , defined in I, for  $q = q'$  and  $p = p'$ . This covariant, which we denote also by  $\Gamma_{\alpha'\alpha}^4$  is

$$\Gamma_{\alpha'\alpha}^4 = -(p'_\alpha kq' - k_\alpha p'q') (p_\alpha kq - k_\alpha pq). \tag{3.1}$$

With (3.1) we obtain for the  $\pi$ -Regge exchange contribution in the non-forward direction ( $k_\perp = k \text{ tg}\theta$ ,  $k'_\perp = k \text{ tg}\theta'$ ):

$$\begin{aligned} H_\pi^{++} &= k'_\perp k_\perp e^{-i(\phi' - \phi)} \zeta_{\alpha\pi}^*(t) \zeta_{\alpha\pi}(t') (s/M^2)^{\alpha_\pi(t') + \alpha_\pi(t)} \\ &\quad \times \text{Im} T_{\pi N}(M^2; t_0, t', t) (F_\pi(q^2))^2, \\ H_\pi^{+-} &= e^{-i(\phi' + \phi)} e^{i(\phi' - \phi)} H_\pi^{++}, \\ H_\pi^{+0} &= -k'_\perp e^{-i\phi'} \zeta_{\alpha\pi}^*(t') \zeta_{\alpha\pi}(t) \left(\frac{s}{M^2}\right)^{\alpha_\pi(t') + \alpha_\pi(t)} \text{Im} T_{\pi N}(M^2; t_0, t', t) \\ &\quad \times (F_\pi(q^2))^2 \sqrt{-q^2} \frac{2\sqrt{2b}}{pq}, \\ H_\pi^{00} &= \zeta_{\alpha\pi}^*(t') \zeta_{\alpha\pi}(t) \left(\frac{s}{M^2}\right)^{\alpha_\pi(t') + \alpha_\pi(t)} \text{Im} T_{\pi N}(M^2; t_0, t', t) \\ &\quad \times (F_\pi(q^2))^2 \left(-4q^2 - \frac{b^2}{pq p'q'}\right). \end{aligned} \tag{3.2}$$

In (3.2) we used the following definitions:

$$\zeta_{\alpha\pi}(t) = \alpha'_\pi \Gamma(-\alpha_\pi(t)) \frac{1}{2} (1 + e^{-i\pi\alpha_\pi(t)}), \tag{3.3}$$

$$b = k_0 |q| + k p_0, \quad (3.4)$$

$$t_0 = (q - q')^2, \quad t = (q - k)^2, \quad t' = (q' - k)^2. \quad (3.5)$$

The off-shell  $\pi N$  amplitude will be approximated by its on-shell expression

$$\text{Im } T_{\pi N}(M^2; t_0, t', t) = (M^2)^{\alpha_P(t_0)} \sigma_{\pi N}^{\text{tot}}(M^2). \quad (3.6)$$

We can accommodate off-shell effects by modifying (3.6) with multiplicative exponential functions of  $t$  and  $t'$ . The variables  $k_\perp$  and  $k'_\perp$  can be expressed by  $\tau$  and  $\tau'$  defined in (2.4):

$$k_\perp = k \text{tg } \theta \approx x\tau, \quad k'_\perp = k \text{tg } \theta' \approx x\tau', \quad (3.7)$$

$$t_0 = -\tau^2 - \tau'^2 + 2\tau\tau' \cos(\phi - \phi'), \quad (3.8)$$

whereas the relation between  $\tau, \tau'$  and  $t, t'$  respectively, was written down in (2.5).

We shall neglect the  $t$ -dependence of the signature factor but retain the  $t$ -dependence of the pion pole, so that  $\zeta_{\alpha_\pi}(t)$  is approximated by

$$\zeta_{\alpha_\pi}(t) \approx \frac{1}{t - m_\pi^2}. \quad (3.9)$$

For the pion pole term we use the following integral representation

$$\frac{1}{m_\pi^2 - t} = \frac{1}{m_\pi^2 - t_{\min}} \int_0^\infty dz e^{-z} e^{-\tau^2 xz / (m_\pi^2 - t_{\min})}. \quad (3.10)$$

By using (3.10) we can perform the integrations in (2.18) analytically since only Gaussian integrals occur. The cut-corrected cross sections are obtained as integrals over  $z$  or/and  $z'$ . To be able to give the result in a concise form we write the  $k_\perp$  factors in the pion Regge amplitudes separately. From (3.2) we have for  $k_\perp = k'_\perp$  and  $\phi = \phi' = 0$ :

$$\begin{aligned} H_\pi^{++}(\tau, \tau) &= k_\perp^2 \widetilde{H}_\pi^{++}(\tau, \tau), \\ H_\pi^{+-}(\tau, \tau) &= k_\perp^2 \widetilde{H}_\pi^{+-}(\tau, \tau), \\ H_\pi^{+0}(\tau, \tau) &= k_\perp \widetilde{H}_\pi^{+0}(\tau, \tau), \\ H_\pi^{00}(\tau, \tau) &= \widetilde{H}_\pi^{00}(\tau, \tau). \end{aligned} \quad (3.11)$$

The result of the integrations in (2.18) appears in the following form:



$$\begin{aligned}
 H^{\lambda\gamma'\lambda\gamma}(\tau, \tau) &= H_{\pi}^{\lambda\gamma'\lambda\gamma}(\tau, \tau) \\
 &+ \widetilde{H}_{\pi}^{\lambda\gamma'\lambda\gamma}(0, 0) \left\{ -(ca) \int_0^{\infty} dz' \int_0^{\infty} dz e^{-(z'+z)} (I_1^{\lambda\gamma'\lambda\gamma}(z', z) + \text{c.c.}) \right. \\
 &\left. + (ca)^2 \int_0^{\infty} dz' \int_0^{\infty} dz e^{-(z'+z)} I_2^{\lambda\gamma'\lambda\gamma}(z', z) \right\}, \tag{3.12}
 \end{aligned}$$

with integrands  $I_1^{\lambda\gamma'\lambda\gamma}(z', z)$  and  $I_2^{\lambda\gamma'\lambda\gamma}(z', z)$  as follows:

$$\begin{aligned}
 I_1^{+-}(z', z) &= I_1^{*-}(z', z) = k_1^2 e^{-\beta_1 \tau^2} \frac{\pi(a+B_v)}{(a+B^*(z')+B_v)^2}, \\
 I_1^{+0}(z', z) &= k_1 e^{-\beta_1 \tau^2} \frac{\pi(a+B_v)}{(a+B^*(z')+B_v)^2}, \\
 I_1^{00}(z', z) &= e^{-\beta_1 \tau^2} \frac{\pi}{a+B^*(z')+B_v}, \tag{3.13}
 \end{aligned}$$

with

$$\beta_1 = B(z) + \frac{B^*(z')(a+B_v)}{a+B^*(z')+B_v}, \tag{3.14}$$

$$\begin{aligned}
 I_2^{++}(z', z) &= \frac{\pi^2}{(D(z', z))^2} e^{-\beta_2 \tau^2} \left\{ x^2 B_v + \frac{a^2 k_1^2 (a+B^*(z')+2B_v)(a+B(z)+2B_v)}{D(z', z)} \right\}, \\
 I_2^{*-}(z', z) &= \frac{\pi^2 a^2 k_1^2}{(D(z', z))^3} (a+B^*(z')+2B_v)(a+B(z)+2B_v) e^{-\beta_2 \tau^2}, \\
 I_2^{+0}(z', z) &= \frac{\pi^2 a k_1}{(D(z', z))^2} (a+B(z)+2B_v) e^{-\beta_2 \tau^2}, \\
 I_2^{00}(z', z) &= \frac{\pi^2}{D(z', z)} e^{-\beta_2 \tau^2}, \tag{3.15}
 \end{aligned}$$

with

$$D(z', z) = (a+B^*(z')+B_v)(a+B(z)+B_v) - B_v^2, \tag{3.16}$$

$$\beta_2 = \frac{a}{D(z', z)} (2B^*(z')B(z) + (B^*(z')+B(z))(a+2B_v)). \tag{3.17}$$

(In (3.12) one of the  $z$ -integration in the interference terms can be trivially performed)

In (3.13) to (3.17) the quantity  $a$  is the exponential slope of the absorptive am-

plitude defined in (2.11) whereas  $B(z)$  is the exponential slope in the  $t$ -channel (see (3.2)) together with the slope of the pion pole term through the integral representation (3.10)

$$B(z) = \left\{ \frac{z}{m_\pi^2 - t_{\min}} + \alpha'_\pi \left( \ln \frac{s}{M^2} - \frac{1}{2} i\pi \right) \right\} x. \quad (3.18)$$

The  $B_v$  is the exponential slope in the  $t_0$  channel (see (3.6)) which for the Pomernchuk exchange is given by

$$B_p = a_p + \alpha'_p \ln M^2. \quad (3.19)$$

In (3.19) we have introduced a constant term  $a_p$  to have the freedom to introduce a  $t$  dependent residue in the Regge exchanges in the  $t_0$  channel. It is well known that for the Pomernchuk such a term is necessary to describe the data for  $\pi N$  scattering.

We see that  $H^{++}$  does not vanish for  $k_\perp^2 = 0$  as expected. The non vanishing term comes from the double-cut contribution. The pole-cut interference term vanishes for  $k_\perp^2 = 0$  similar to the pure pole term. For small  $k_\perp$  the pole-cut interference term is negative. Thus for an appropriate value for  $c$  we can expect that the terms proportional to  $k_\perp^2$  (the pure pole term,  $I_1$  and the term in  $I_2$ ) can be minimized. The combination  $\frac{1}{2}(H^{++} + H^{+-})$  which is proportional to the transversely polarized cross section  $\sigma_\perp$ , is particularly simple and is completely given by the double-cut term, namely

$$\frac{1}{2}(H^{++} + H^{+-}) = (ca)^2 \int_0^\infty dz' \int_0^\infty dz e^{-(z+z')} \frac{\pi^2 x^2 B_v}{(D(z', z))^2} e^{-\beta_2 k_\perp^2/x^2} \tilde{H}_\pi^{++}(0, 0). \quad (3.20)$$

We see that the cross section  $\sigma_\perp$  vanishes for  $x \rightarrow 0$  like  $x^2$  if  $k_\perp = 0$ , and in a more complicated form for  $k_\perp \neq 0$ . Furthermore we remark that the longitudinal cross section is affected by cut terms much less than the other cross sections.

### 3.2. $\omega$ -exchange

We study  $\omega$  exchange in order to calculate the cross section for  $\pi^0$  inclusive production. It is clear that the results can also be used for  $\rho$  exchange and  $A_2$  exchange with appropriate changes of notation.

For  $\omega$  exchange we have no problem with gauge invariance since it is explicitly gauge invariant. As input we need the imaginary part of the off-shell  $\omega N$  scattering amplitude for non-forward angles. Even the nucleon spin averaged part consists of many terms. For small scattering angles they produce comparable contributions. It would be a too lengthy calculation to incorporate all possible terms. Furthermore we have no information about their relative size. Therefore we take for  $\text{Im } T_{\mu\nu}^{\omega N}$ , the simple form

$$\text{Im } T_{\mu\nu}^{\omega N} = V_1 p'_\mu p_\nu. \quad (3.21)$$

Terms proportional to  $g_{\mu\nu}$  do not contribute in the high energy limit as was found

in I. With (3.21) we have calculated explicitly  $H_{\omega}^{++}$  and  $H_{\omega}^{+-}$  for different  $k_{\perp}$  and  $k'_{\perp}$ . The result is:

$$\begin{aligned}
 H_{\omega}^{++} &= \frac{1}{8} F_{\omega\pi\gamma}^2 (q^2) \zeta_{\alpha_{\omega}}(t) \zeta_{\alpha_{\omega}}^*(t) \left(\frac{s}{M^2}\right)^{\alpha_{\omega}(t) + \alpha_{\omega}(t')} M^4 V_1(M^2, t_0, t', t) k'_{\perp} k_{\perp} e^{-i(\phi' - \phi)}, \\
 H_{\omega}^{+-} &= H_{\omega}^{++} e^{-2i\phi}.
 \end{aligned}
 \tag{3.22}$$

This agrees with (3.18) in I if  $k_{\perp} = k'_{\perp}$ ,  $\phi = \phi' = 0$ . Of course the other amplitudes  $H_{\omega}^{+0}$  and  $H_{\omega}^{00}$  vanish in the high energy limit. For estimates of cross sections we shall approximate  $M^4 V_1$  by the imaginary part of the off-shell pion-nucleon scattering amplitude.

$$M^4 V_1(M^2, t_0; t', t) \approx \text{Im } T^{\pi N}(M^2, t_0; t', t).
 \tag{3.23}$$

Except from  $t$  and  $t'$  independent factors the structure of  $H_{\omega}^{++}$  and  $H_{\omega}^{+-}$  is the same as that of  $H_{\pi}^{++}$  and  $H_{\pi}^{+-}$  except that the  $\pi$  and  $\omega$  trajectories are different. For the  $\omega$  trajectory the signature factor can be taken as constant except for the  $t$  dependent phase factor:

$$\begin{aligned}
 \zeta_{\alpha_{\omega}}(t) &= e^{-\frac{1}{2}i\pi\alpha_{\omega}(t)} i \frac{\pi\alpha'_{\omega}}{\Gamma(\alpha_{\omega}(t) + 1) \sin \pi\alpha_{\omega}(t)} \\
 &\approx e^{-\frac{1}{2}i\pi\alpha_{\omega}(t)} i \frac{\pi\alpha'_{\omega}}{\Gamma(\alpha_{\omega}(0) + 1) \sin \pi\alpha_{\omega}(0)}.
 \end{aligned}
 \tag{3.24}$$

Thus for the  $\omega$  signature factor we do not need the integral representation (3.10). Then the cut contributions are obtained explicitly without further integrations. The results can be read off from (3.12) to (3.17) by removing the  $z$  integration and re-defining  $B$  according to

$$B = \{b + \alpha'_{\omega} (\ln \frac{s}{M^2} - \frac{1}{2}i\pi)\} x.
 \tag{3.25}$$

One obtains for  $H^{\lambda'\gamma\lambda\gamma}$  the expression

$$\begin{aligned}
 H^{\lambda'\gamma\lambda\gamma}(\tau, \tau) &= H_{\omega}^{\lambda'\gamma\lambda\gamma} + \tilde{H}_{\omega}^{\lambda'\gamma\lambda\gamma}(0, 0) \\
 &\times \{-(ca)(I_1^{\lambda'\gamma\lambda\gamma} + \text{c.c.}) + (ca)^2 I_2^{\lambda'\gamma\lambda\gamma}\},
 \end{aligned}
 \tag{3.26}$$

where

$$I_1^{++} = I_1^{+-} = k_{\perp}^2 e^{-\delta_1 \tau^2} \frac{\pi(a+B)}{(a+B^* + B_{\nu})^2},
 \tag{3.27}$$

with

$$\delta_1 = B + \frac{B^*(a+B_{\nu})}{a+B^* + B_{\nu}},
 \tag{3.28}$$

$$I_2^{++} = \frac{\pi^2}{D^2} e^{-\delta_2 \tau^2} \left\{ x^2 B_v + a^2 k_\perp^2 \frac{(a+B^*+2B_v)(a+B+2B_v)}{D} \right\}, \quad (3.29)$$

$$I_2^{+-} = \frac{\pi^2 a^2 k_\perp^2}{D^3} e^{-\delta_2 \tau^2} (a+B^*+2B_v)(a+B+2B_v),$$

with

$$D = |a+B+B_v|^2 - B_v^2, \\ \delta_2 = \frac{a}{D} (2|B|^2 + (B^*+B)(a+2B_v)). \quad (3.30)$$

As one expects we see that  $\frac{1}{2}(H^{++} - H^{+-}) \sim \sigma_{\parallel}$  is completely determined by the double-cut term, namely

$$\frac{1}{2}(H^{++} - H^{+-}) = \tilde{H}_{\omega}^{++}(0,0) (ca)^2 \frac{\pi^2 x^2}{D^2} e^{-\delta_2 k_\perp^2/x^2}. \quad (3.31)$$

Except for the integration over  $z$  and  $z'$  this has the same structure as  $\sigma_{\perp}$  for one-pion exchange (see (3.25)), it vanishes like  $x^2$  for  $x \rightarrow 0$  and  $k_\perp = 0$ . If in a model using Regge poles, we define  $\alpha'_R$  and  $\alpha'_v$  to be the  $t$ -slopes of the Reggeons in the  $t$ - and  $t_0$ -channels respectively and  $\alpha'_p$  to be the  $t$ -slope of the pomeron in the initial  $\gamma P$  channel, then we can calculate the  $t = -xk_\perp^2$  slope of the cut  $\alpha'_c$ , using the substitutions

$$B = x\alpha'_R \ln s/M^2, \quad B_v = \alpha'_v \ln M^2, \quad a = a_p + \alpha'_p \ln s. \quad (3.32)$$

In the limit  $s \rightarrow \infty$ ,  $M^2$  fixed ( $x \simeq 1$ ), one obtains

$$\alpha'_c = \frac{\alpha'_p \alpha'_R}{\alpha'_p + \alpha'_R}, \quad (3.33)$$

while in the limit  $s \rightarrow \infty$ ,  $(s/M^2) \ll s$  ( $x \ll 1$ ) one obtains

$$\alpha'_c = \alpha'_R. \quad (3.34)$$

#### 4. Discussion and conclusions

Using the results of sect. 3 we have calculated the Regge pole plus cut contributions for various values of the absorption parameter  $c$ . In fig. 4 we show a comparison of the  $k_\perp^2$  dependence of the  $\gamma p \rightarrow \pi^- x$  distribution with the data of Moffeit et al. [13] at  $E_\gamma = 9.3$  GeV. The  $c = 2$  curve reproduces the data at this energy quite well, in particular the peak-shoulder structure in the region  $0 < k_\perp^2 < 0.1$  GeV<sup>2</sup>. On the other hand the value  $c = 2.6$  reproduces the data of Burfeindt et al. [14] at the lower energy  $E_\gamma = 3.2$  GeV (fig. 5). The non-vanishing of the cross section with  $k_\perp^2$

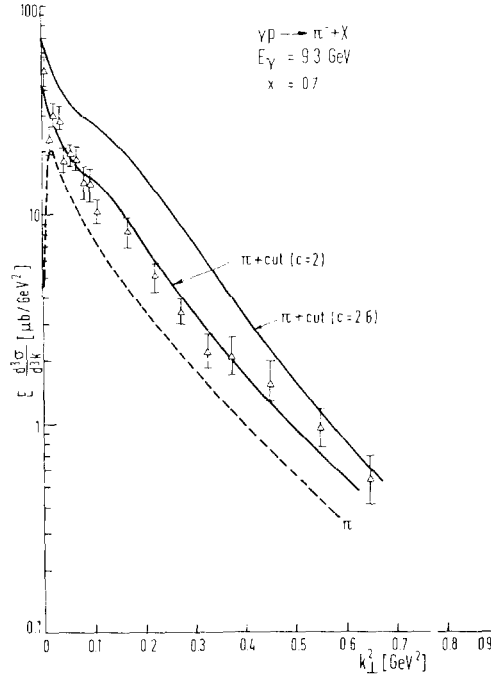


Fig. 4. Data for  $\gamma p \rightarrow \pi^- x$  from Moffeit et al. [13], compared to the theoretical curves with  $c = 2$  and  $c = 2.6$ . The dotted curve is the pion pole contribution.

is more marked in this data, for which  $k_{\perp}^2 \simeq 0.01 x^2 \lesssim 0.5 m_{\pi}^2$ , we see that both  $\pi^+$  and  $\pi^-$  distributions are reproduced with  $c \simeq 2.6$  except near  $x \simeq 0.9$ , where one has to properly take care of the  $\Delta_{33}$  contribution (see ref. [1]).

The variation of  $c$  with energy may indicate that multiple-pomeron-exchange is relevant at these energies. A nice test of the detailed dynamics would be obtained from a measurement of  $\sigma_{\parallel}$  and  $\sigma_{\perp}$  separately. For example  $\sigma_{\perp}$  is given entirely in terms of the double cut contribution and leads to the exponentially falling curve in fig. 6. In contrast  $\sigma_{\parallel}$  shows a marked interference structure. This is responsible for the shoulder in  $\sigma_{\perp}$ .

Similarly the calculation for neutral pion inclusive photoproduction is compared with the data of Berger et al. [15] in fig. 7, where we again plot the distribution in  $k_{\perp}^2$ . Here the two curves for  $x = 0.86$  and  $x = 0.64$  are shown with  $c = 0.7$ . The data for the larger  $x$  is adequately reproduced with this value of  $c$ . However there is a deviation from the data of smaller  $x$ , which might be expected from the kinematic limitations on the triple-Regge expansion and the likelihood that the photon and target fragmentation regions overlap at these energies. For  $x > 0.7$  a good test of the modified triple Regge dynamics we have considered, would be again to measure  $\sigma_{\parallel}$  and  $\sigma_{\perp}$  individually. In this case the double cut contributes only to  $\sigma_{\parallel}$  and  $\sigma_{\perp}$  shows a

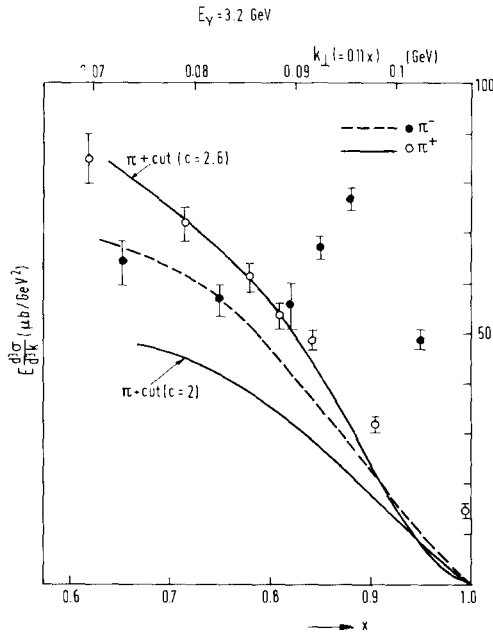


Fig. 5. Comparison of the model with  $c = 2$  and  $2.6$  respectively with the small  $k_{\perp}^2$  data ( $k_{\perp} = 0.11x$ ) of Burfeindt et al. [14]. (The dotted curve shows the prediction for  $\gamma p \rightarrow \pi^- X$ ).

marked interference structure (fig. 8). It is interesting to compare figs. 6 and 8, when one sees some differences in the small  $k_{\perp}^2$  behaviour. In particular we notice the expected difference in the scale as reflected for example in the position of the

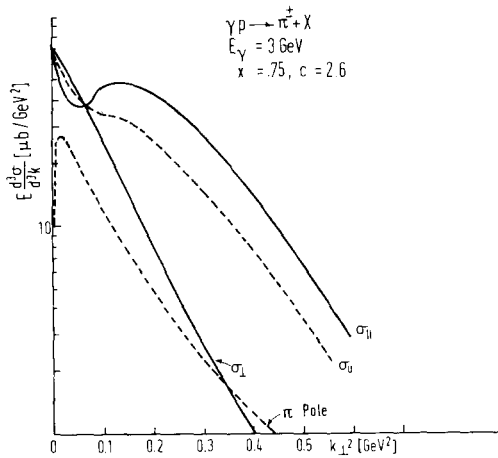


Fig. 6. A plot of the dependence of  $\sigma_{\parallel}$ ,  $\sigma_{\perp}$  and  $\sigma_{\cup}$  and the pole term as a function of  $k_{\perp}^2$ .

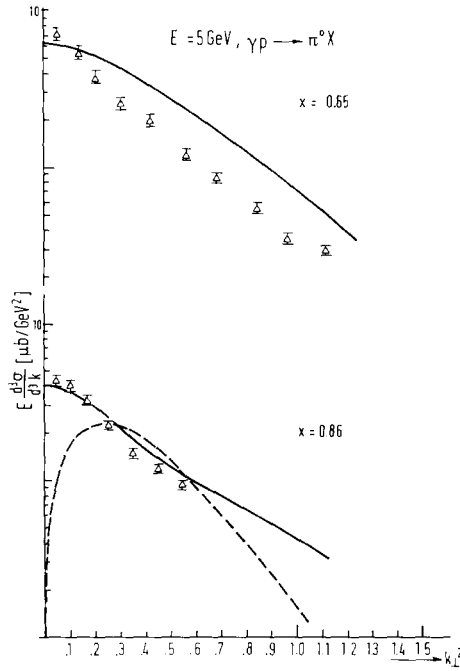


Fig. 7. Comparison of the model with the data of Berger et al. [15] on  $\gamma p \rightarrow \pi^0 X$ . (The dotted line represents the  $\omega$  exchange term and the solid curve corresponds to  $c = 0.7$ ).

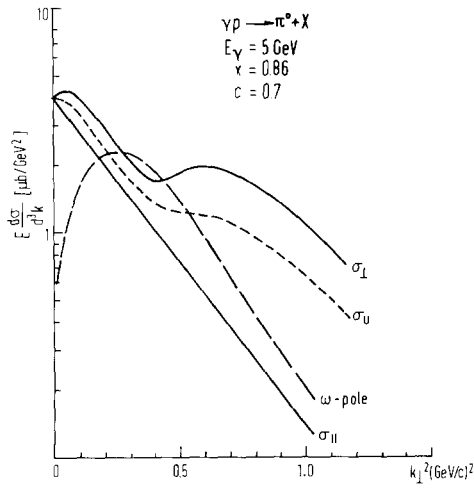


Fig. 8. The dependence of  $\sigma_{\parallel}$ ,  $\sigma_{\perp}$ ,  $\sigma_U$  and the  $\omega$ -pole term on  $k_{\perp}^2$ .

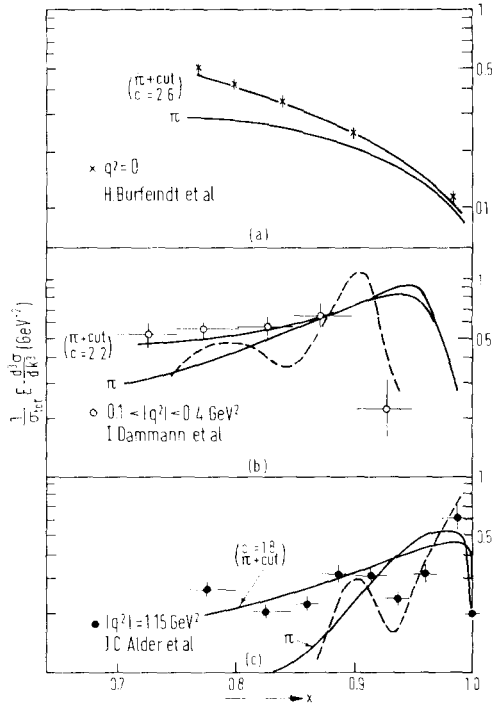


Fig. 9. Comparison of the Mueller Regge model for  $q^2 = 0.0, 0.2$  and  $1 \text{ GeV}^2$  with the  $x$  distribution of the inclusive data for  $\gamma p \rightarrow \pi^+ x$  from ref. [16].

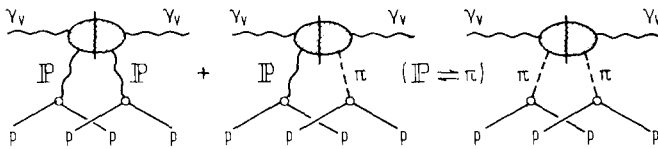


Fig. 10. Triple Regge expansion of  $\gamma_V p \rightarrow p x^0$ .

dip. This comes from the sharp variation in the pion propagator as a function  $k_{\perp}^2$  in the case of charged pion production.

The electroproduction of charged pions has also been calculated for various values

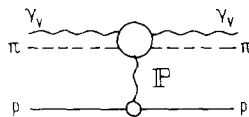


Fig. 11. Full Mueller Regge diagram of  $\gamma_V p \rightarrow \pi x$  in the photon fragmentation region ( $x > 0$ ).



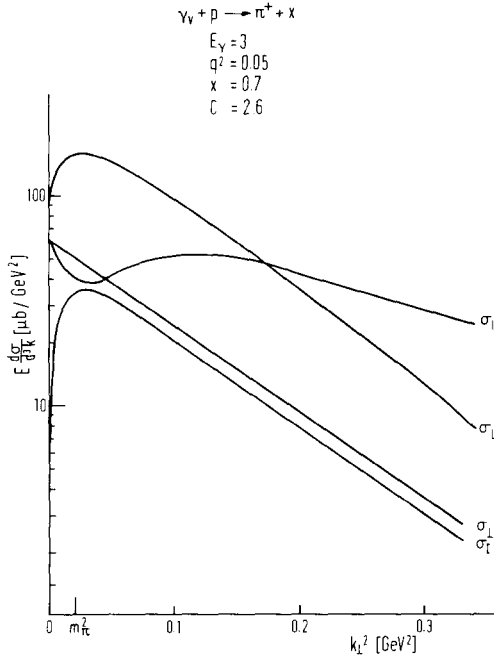


Fig. 12. Plot of  $\sigma_{||}$ ,  $\sigma_{\perp}$ ,  $\sigma_L$  and  $\sigma_T$  for  $\gamma p \rightarrow \pi^+ x$  as a function of  $k_{\perp}^2$  in the transitional region  $q^2 \simeq 0.05$ .

of  $q^2$  and compared with the data [16] in fig. 9. The conclusion in (I), that for  $q^2 > 0.1 \text{ GeV}^2$  the charged distributions are predominantly longitudinal is unchanged by the addition of the cuts. We see that Regge cuts smear out the  $x$  distributions, which for the pion pole, is dictated by the dependence of the pion propagator on  $x$  and  $q^2$ , namely

$$x^2 / [(1-x) + (m_{\pi}^2 + k_{\perp}^2) / (-q^2)]^2.$$

The broader distributions agree better with the data. In the calculation we use, for  $q^2 = 0, 0.3$  and  $1 \text{ GeV}^2$ , the values of  $c = 2.6, 2.2$  and  $1.8$  respectively. A dependence of  $c$  on  $q^2$  is expected and in principle could be extracted from the  $q^2$  dependence of  $\gamma_V + p \rightarrow p + x^0$ , which will receive an important contribution from the interference term shown in fig. 10. However, we see that the larger  $q^2$  data [17] in the region  $0 < x < 0.8$  is not easily explained within the triple Regge framework. The reason is the dependence on the particle-Reggeon form factors, which for fixed mass are expected always to be rapidly decreasing functions of  $q^2$ . Presumably for larger  $q^2$  the triple Regge mechanism becomes an increasingly poor approximation to fig. 11.

We finally remark on the behaviour of  $\sigma_{||}$ ,  $\sigma_{\perp}$ ,  $\sigma_L$  and  $\sigma_T$  in the transition region

$q^2 \sim m_\pi^2$ , which is indicated in fig. 12 for  $q^2 = 0.05 \text{ GeV}^2$ . In particular one sees that the interference term  $\sigma_I$  is only large in this very narrow region. This demonstrates how the electroproduction can change very rapidly as a function of  $q^2$ , when we go to the photoproduction limit, in contrast to the smooth limiting behaviour proposed by Bjorken and Kogut [11]. Presumably this small  $q^2$  range would be a sensitive region, in which the Mueller-Regge-expansion discussed in this paper can be tested.

## Appendix A

Here we derive the representation (2.4) and its inverse (2.5) from (2.1). We begin by explicitly exhibiting the summation over the total helicity  $\lambda_x$  of the missing mass state  $x$ . Denoting the total angular momentum of  $x$  by  $s_x$  and all the other labels including the degeneracy by  $\eta_x$ , we can write the summation over  $\xi$  defined in (2.1) by

$$\begin{aligned} & \sum_{\xi} \int \prod_1^n \frac{d^3 k_i}{(2\pi)^3 2k_{i0}} (2\pi)^4 \delta^{(4)} \left( \sum_1^n k_j + k - p - q \right) |k, k_1, \dots, k_n\rangle \langle k, k_1, \dots, k_n| \\ & = \sum_{s_x, \lambda_x, \eta_x} |k, p_x, s_x, \lambda_x, \eta_x\rangle \langle k, p_x, s_x, \lambda_x, \eta_x|. \end{aligned} \quad (\text{A.1})$$

On inserting (A.1) in (2.1), we can partial-wave analyze the matrix elements with the result:

$$\begin{aligned} H^{\lambda'\lambda} & = \sum_{m=\lambda_x+\lambda_p}^{\infty} \sum_{\substack{J=\text{Max}\{|\lambda_x|, |\lambda-\lambda_p|\} \\ J'=\text{Max}\{|\lambda_x|, |\lambda'-\lambda_p|\}}} \frac{(2J+1)}{4\pi} \frac{(2J'+1)}{4\pi} D_{\lambda-\lambda_p, \lambda_x}^J(\phi, \theta, -\phi) \\ & \times D_{\lambda_x, \lambda'-\lambda_p}^{J'*}(\phi', \theta', -\phi') \sum_{n, s_x, \eta_x} \langle \lambda', \lambda_p | T_n^J(s, M^2) | s_x', \lambda_x, \eta_x \rangle \\ & \times \langle s_x, \lambda_x, \eta_x | T_n^{J'}(s, M^2) | \lambda, \lambda_p \rangle \\ & = \sum_{m=-\infty}^{+\infty} e^{i(m+\lambda)\phi} e^{-i(m+\lambda')\phi'} H_m^{\lambda\lambda'}(s, M^2, \cos\theta, \cos\theta'), \end{aligned} \quad (\text{A.2})$$

where

$$\begin{aligned} H_m^{\lambda'\lambda} & = \sum_{\substack{J=\text{Max}\{|m-\lambda_p|, |\lambda-\lambda_p|\} \\ J'=\text{Max}\{|m-\lambda_p|, |\lambda'-\lambda_p|\}}} \frac{(2J+1)}{4\pi} \frac{(2J'+1)}{4\pi} d_{\lambda-\lambda_p, m-\lambda_p}^J(\theta) \\ & \times d_{m-\lambda_p, \lambda'-\lambda_p}^{J'}(\theta') h_m^{\lambda\lambda'}(J, J'), \end{aligned} \quad (\text{A.3})$$

with

$$h_m^{\lambda'\lambda} = \sum_{n, s_X, \eta_X} \langle \lambda', \lambda_p | T_n^J | s_X, m - \lambda_p, \eta_X \rangle \langle s_X, m - \lambda_p, \eta_X | T_n^{J'} | \lambda, \lambda_p \rangle. \tag{A.4}$$

One obtains an impact parameter representation by using the approximation

$$d_{\lambda\mu}^J(\theta) \simeq J_{|\lambda-\mu|}((2J+1) \sin \frac{1}{2}\theta), \tag{A.5}$$

and by defining the variables,

$$b = q^{-1}(J + \frac{1}{2}), \quad \tau = 2q \sin \frac{1}{2}\theta. \tag{A.6}$$

The result is

$$H_m^{\lambda'\lambda} = \int_{b'_m}^{\infty} db' b' \int_{b_m}^{\infty} db b J_{m+\lambda}(b'\tau) J_{m+\lambda}(b\tau) h^{\lambda'\lambda}(b', b; m), \tag{A.7}$$

where

$$b_m = \frac{1}{q} [\text{Max} \{ |m - \lambda_p|, |\lambda - \lambda_p| \} + \frac{1}{2}].$$

When one examines the kinematic singularities of the *D*-functions, which have to be compensated by corresponding factors in the amplitude one finds that

$$h^{\lambda'\lambda}(b, b'; m) \simeq (bb')^m \text{ as } b, b' \rightarrow 0. \tag{A.8}$$

Hence at high energies the lower limit  $b_m \sim m/\sqrt{s}$  can be set equal to zero provided  $m < \sqrt{s}$  i.e., summation over  $m$  converges sufficiently fast.

### Appendix B

We provide here an alternative method of deriving (2.13) based on analyzing Regge diagrams in the triple-Regge limit. We illustrate the method by considering the double Regge cut diagram shown in fig. 13, which can be represented by the ex-

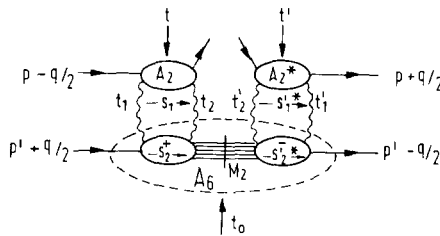


Fig. 13. Reggeon diagram for the double-cut contribution.

pression (neglecting helicity)

$$\begin{aligned}
 H = & \int \frac{d^4 k}{(2\pi)^4} A_2^{\alpha_1 \alpha_2}(s_1, t_1, t_2, t) \left[ \frac{s}{s_1 s_2} \right]^{\alpha_1(t_1)} \left[ \frac{s}{(M^2 + s_2) s_1} \right]^{\alpha_2(t_2)} \\
 & \times \int \frac{d^4 k'}{(2\pi)^4} A_2^{\alpha_1 \alpha_2^*}(s_1^*, t_1', t_2', t') \left[ \frac{s}{s_1^* s_2^*} \right]^{\alpha_1(t_1')} \left[ \frac{s}{(M^2 + s_2^*) s_1^*} \right]^{\alpha_2(t_2')} \\
 & \times \text{Disc}_{M^2} A_6^{\alpha_1 \alpha_2}(s_2, s_2^*, M^2, t_1, t_2, t, t_1', t_2', t', t_0).
 \end{aligned} \tag{B.1}$$

The standard procedure [12] is to convert the loop integral over  $d^4 k$  to an integral over the reggeon mass variable  $t_1 = k^2, t_2 = (k-q)^2$  and the channel invariants  $s_1 = (p - \frac{1}{2}q - k)^2$  and  $s_2 = (p' + \frac{1}{2}q + k)^2$  defined in fig. 13

$$\begin{aligned}
 d^4 k &= J dt_1 dt_2 ds_1 ds_2, \\
 J &= 4 \begin{vmatrix} p^2 & p \cdot p' & p \cdot q & p \cdot k \\ p \cdot p' & p'^2 & p' \cdot q & p' \cdot k \\ p \cdot q & p' \cdot q & q^2 & q \cdot k \\ p \cdot k & p' \cdot k & k \cdot q & k^2 \end{vmatrix}^{-\frac{1}{2}}
 \end{aligned} \tag{B.2}$$

(a) In the limit  $s \rightarrow \infty, M^2, s_1, s_1$  fixed;

$$\begin{aligned}
 J &= 4s^{-1} [(q \cdot k)^2 - k^2 q^2]^{-\frac{1}{2}} \\
 &= s^{-1} \lambda^{-\frac{1}{2}}(t_1, t_2, t), \\
 d^4 k &\rightarrow (1/s) d^2 \tau ds_1 ds_2,
 \end{aligned}$$

where

$$t_1 = \tau'^2, \quad t_2 = (\tau - \tau')^2, \quad t = \tau^2. \tag{B.4}$$

(b) In the limit  $(s/M^2) = (1-x)$  fixed,  $s \rightarrow \infty, s_1, s_2$  fixed;

$$J = 4s^{-1} [(k \cdot Q)^2 - k^2 Q^2]^{-\frac{1}{2}},$$

where

$$Q = (1+x)q/2 + (1-x)p, \quad Q^2 = xq^2 = xt. \tag{B.5}$$

Defining

$$t_1 = \tau'^2, \quad t_2 = (\tau - \tau')^2/x, \quad t = \tau^2/x,$$

then

$$d^4k \rightarrow d^2\tau' ds_1 ds_2. \tag{B.6}$$

Providing the singularity structure of the amplitudes in the channel variables  $s_1$  and  $s_2$  etc. have the necessary left-right singularity structure, for case (b) we can rewrite  $H$  in the following form

$$H = \int \frac{d^2\tau'}{(2\pi)^2} \int \frac{d^2\tau''}{(2\pi)^2} N(\tau, \tau') N^*(\tau, \tau'') s^{\alpha_1(\tau'^2) + \alpha_1(\tau''^2) - 1} \times \left(\frac{s}{M^2}\right)^{\alpha_2([\tau - \tau']^2/x) + \alpha_2([\tau - \tau'']^2/x)} \text{Disc}_{M^2} T^{\alpha_1\alpha_2}(M^2, t_1, t_2, t, t'_1, t'_2, t', t_0), \tag{B.7}$$

where

$$N(\tau, \tau') = \beta^{\alpha_1}(t_1) \beta^{\alpha_2}(t_2) + \int_{s_0}^{\infty} ds_1 \text{Im} A_2^{\alpha_1\alpha_2}(s_1, t_1, t_2, t), \tag{B.8}$$

$$\text{Disc}_{M^2} T^{\alpha_1\alpha_2} = \beta^{\alpha_1'}(t_1) \beta^{\alpha_1'}(t'_1) \text{Disc}_{M^2} T_6^{\alpha_2}(M^2, t_2, t_2, t_0) \tag{B.9}$$

+ terms involving discontinuities of  $A_6$  in the variables  $s_2, s'_2$ .

In (B.8) and (B.9) we have explicitly extracted the pole contributions in the variable  $s_1$  and  $s_2$ . These terms lead to the reggeon diagrams shown in fig. 3 for  $\gamma p \rightarrow \pi + x$ . (The continuum contributions are estimated by inserting a multiplicative factor as a first approximation see (sect. 3)).

### References

- [1] N.S. Craigie, J. Körner and G. Kramer, Nucl. Phys. B68 (1974) 509.
- [2] P.D.B. Collins, Phys. Reports 1 (1971) 103.
- [3] P. Stichel, Z. Phys. 180 (1964) 170;  
G. Cohen-Tannoudji, Ph. Salin and A. Morel, Nuovo Cimento 55A (1968) 412.
- [4] B. Richter, Proc. of the 1967 Int. Symposium on electron and photon interactions, Stanford  
K. Lübelmeyer, Proc. of the 4th Int. Symposium on electron-photon interactions at high energies 1969, Daresbury.
- [5] G. Kramer, K. Schilling and L. Stodolsky, Nucl. Phys. B5 (1968) 317.
- [6] M.K. Blackmon, G. Kramer and K. Schilling, Nucl. Phys. B12 (1969) 495;  
R. Worden, Nucl. Phys. B37 (1972) 253.
- [7] F. Brasse, Proc. of Int. Symposium on electron-photon interactions at high energies 1973, Bonn, DESY report DESY 73/49.
- [8] A.H. Mueller, Phys. Rev. D2 (1970) 2963;  
P. Goddard and A.R. White, Nuovo Cimento 1A (1971) 645;  
C.E. de Tar and J.H. Weis, Nuovo Cimento D6 (1971) 3141;  
C.E. Jones, F.E. Low and J.E. Young, Phys. Rev. D4 (1973) 2358;  
H.D.I. Abarbanel and A. Schwimmer, Phys. Rev. D6 (1971) 3018.

- [9] N.S. Craigie and G. Kramer, in preparation.
- [10] J. Cardy, preprint TH. 1625, CERN (Feb. 1973).
- [11] J.D.B. Bjorken and J. Kogut, Phys. Rev. D8 (1973) 1341.
- [12] (a) H. Rothe, Phys. Rev. 159 (1971) 471;  
(b) N.S. Craigie and Alberto de la Torre, Nucl. Phys. B55 (1973) 551.
- [13] K.C. Moffeit et al., Phys. Rev. D5 (1972) 1603.
- [14] H. Burfeindt et al., Phys. Letters B43 (1973) 345.
- [15] C. Berger et al., Phys. Letters B47 (1973) 377.
- [16] I. Dammann et al., Nucl. Phys. B54 (1973) 381;  
J.C. Alders et al., Nucl. Phys. B46 (1972) 145.
- [17] L. Ahrens et al., Cornell preprint, CLNS-255 (Nov. 1973).